Antifungal tolerance and resistance emerge at distinct drug concentrations and rely upon different aneuploid chromosomes

Feng Yang[a,b], Eduardo FC Scopel[b], Hao Li[a,c], Liu-liu Sun[a,c], Nora Kawar[b], Yong-bing Cao[d], Yuan-Ying Jiang[a,#], Judith Berman[b,#]

[a]Department of Pharmacy, Shanghai Tenth People's Hospital, School of Medicine, Tongji University, Shanghai, China

[b]Shmunis School of Biomedical and Cancer Research, The George S. Wise Faculty of Life Sciences, Tel Aviv University, Tel Aviv, Israel

[c]Department of Physiology and Pharmacology, School of Basic Medicine and Clinical Pharmacy, China Pharmaceutical University, Nanjing, China

[d]Department of Vascular Disease, Shanghai TCM-Integrated Hospital, Shanghai University of Traditional Chinese Medicine, Shanghai, China

[#]Address correspondence to jberman@tauex.tau.ac.il (J.B), and jiangyy@tongji.edu.cn (Y-y. J)

Abstract

Antifungal drug tolerance is a response distinct from resistance, in which cells grow slowly above the minimum inhibitory drug concentration (MIC). Here we found that the majority (69.2%) of 133 *Candida albicans* clinical isolates, including standard lab strain SC5314, exhibited *temperature-enhanced* tolerance at 37˚C and 39°C, and were not tolerant at 30°C. Other isolates were either *always* tolerant (23.3%) or *never* tolerant (7.5%) at these three temperatures, suggesting that tolerance requires different physiological processes in different isolates. At supra-MIC fluconazole concentrations (8-128 µg/ml), tolerant colonies emerged rapidly at a frequency of ~10^{-3}. In liquid passages over a broader range of fluconazole concentrations (0.25-128 µg/ml), tolerance emerged rapidly (within one passage) at supra-MIC concentrations. By contrast, resistance appeared at sub-MIC concentrations after 5 or more passages. Of 155 adaptors that evolved higher tolerance, all carried one of several recurrent aneuploid chromosomes, often including chromosome R, alone or in combination with other chromosomes. Furthermore, loss of these recurrent aneuploidies was associated with a loss of acquired tolerance, indicating that specific aneuploidies confer fluconazole tolerance. Thus, genetic background and physiology, and the degree of drug stress (above or below the MIC) influence the evolutionary trajectories and dynamics with which antifungal drug resistance or tolerance emerges.

Introduction

More than 1.5 million people die from invasive fungal infections every year (Bongomin, et al. 2017). Increases in the global prevalence of fungal infections has become a major public health concern (Enoch, et al. 2017). This is largely because the at-risk population is expanding with the increase in patients with compromised immunity, who are especially vulnerable to fungal infection and the overall increase in lifespan in general. For the vast majority of fungal infections, high morbidity and mortality are caused by species from the genera *Candida*, *Aspergillus* and *Cryptococcus* species (Bongomin, et al. 2017).

Only three antifungal drug classes are used clinically for monotherapy: the polyenes, azoles and echinocandins (Robbins, et al. 2017). Polyenes, such as amphotericin B, have potent and broad-spectrum antifungal activity and resistance is rarely seen. However, polyenes can cause severe toxicity in the kidneys and the liver (Carolus, et al. 2020), because they also bind to human cholesterol. Echinocandins are fungicidal against most *Candida* species and are first-line drugs for the treatment of candidemia (Pappas, et al. 2016). However, the relatively high cost of echinocandins and the need to administer them intravenously, makes them inappropriate in many settings. Azoles, such as fluconazole (FLC), inhibit 14α-lanosterol demethylase, a key enzyme in ergosterol biosynthesis. Azoles, which are fungistatic, have broad-spectrum antifungal activity, good safety profiles, relatively high bioavailability and are more affordable in many healthcare settings. Therefore, azoles are one of the most widely used antifungal drugs (Roemer and Krysan 2014; Robbins, et al. 2016).

The clinical prevalence of FLC resistance in *C. albicans,* a prevalent opportunistic human fungal pathogen, is generally less than 1% (Pfaller, et al. 2019). Despite this, therapeutic failure of FLC against susceptible *C. albicans* isolates is often >30% in systemic infections (Levinson, et al. 2021). The fungistatic nature of azoles allows cells to survive and to evolve new traits, such as drug tolerance or resistance.

Since the introduction of first-generation azole drugs in the 1990s, most published research on drug responses did not distinguish between resistance and tolerance. Antifungal drug tolerance, which is distinct from resistance, has been best characterized in *C. albicans* cells responding to FLC ((Rosenberg, et al. 2018) and reviewed in (Berman and Krysan 2020)). Antifungal drug resistance is the ability to grow well at drug concentrations above a defined MIC for the drug. Antifungal drug tolerance is defined as a characteristic of drug-susceptible genotypes that can grow, albeit slowly, at inhibitory drug concentrations (Fisher, et al. 2022). Furthermore, in a tolerant isolate, not all cells in the isogenic population grow with similar dynamics. Furthermore, individual clinical isolates exhibit different levels of FLC tolerance, and the degree of tolerance changes as a function of growth conditions (Rosenberg, et al. 2018; Levinson, et al. 2021). However, the degree to which tolerance in different isolates varies across environmental conditions remains to be characterized.

Mechanistically, antifungal resistance is usually due to genetic/genomic mutations that directly affect the drug-target interaction and these mutations affect the response of all cells in a population. Antifungal drug tolerance depends upon diverse stress pathway responses, including heat-shock responses, responses to amino acid starvation, kinases such as protein kinase C, and epigenetic processes (Berman and Krysan 2020). Stress pathways presumably enable the slow growth of some cells, and likely affect drug-target interactions indirectly. However, the mechanisms that affect tolerance and that distinguish tolerance and resistance are not well understood. Because the persistence and mortality of fungal infections is associated with high levels of tolerance (Rosenberg, et al. 2018; Levinson, et al. 2021), we posit that antifungal tolerance, a property often overlooked in clinical assays, may explain at least some of the treatment failures caused by clinical isolates that test as susceptible. We also hypothesize that understanding how genetic and physiological processes that modulate tolerance should identify new strategies to improve the outcomes of antifungal drug therapies.

In this study, we first screened a collection of 133 clinical isolates to determine the prevalence of FLC tolerance under in vitro lab conditions at normal and at febrile body

105 temperatures. We found three distinct types of temperature responses: 1) *temperature-*
106 *elevated tolerance* (TET) at 37 and 39°C, relative to 30°C; 2) *always-tolerant* (AT) and
107 never-tolerant (NT) isolates at the three temperatures. We then evolved representative
108 TET and AT isolates for adaptation to FLC at a range of drug concentrations. We found
109 that aneuploidy appears rapidly and is associated with increased tolerance, especially
110 at drug concentrations above the MIC. By contrast, resistant isolates emerged at sub-
111 MIC drug concentrations, only after ~5 days of passaging in sub-MIC drug
112 concentrations and they proceeded to acquire higher resistance levels with time. Some
113 of the resistant adaptors also acquired aneuploidies, but different ones from those in
114 tolerant adaptors. This suggests that tolerance and resistance appear with distinct
115 evolutionary dynamics and trajectories.
116
117

Results

Most clinical isolates tested were fluconazole-tolerant at physiologically relevant temperatures

Previously, we found that temperature and medium composition each affected antifungal tolerance to fluconazole (FLC) and ketoconazole (Rosenberg, et al. 2018; Xu, et al. 2021). Therefore, we asked about how these two physiological factors affected one another. Interestingly, the effect of temperature on FLC tolerance was modulated, sometimes in opposite ways, by medium composition. For example, on RPMI-1640 and casitone plates, SC5314 was tolerant at *both* 30˚C and 37˚C, yet on chromagar, SD or SDC plates, the same strain was not tolerant at *either* 30˚C or 37 ˚C. Interestingly, on YPD medium (a nutrient-rich medium), SC5314 had *temperature-enhanced* tolerance: it was *non-tolerant* at 30˚C and *tolerant* at 37˚C (Fig. S1). Thus, FLC tolerance is regulated by the interplay between temperature and medium composition.

To determine the role of temperature in tolerance across a broader set of clinical isolates, we surveyed 133 clinical *C. albicans* isolates for their susceptibility/resistance and tolerance levels in YPD medium under standard lab conditions (30°C) and at normal (37°C) and febrile (39°C) human body temperatures. We used disk diffusion assays (DDA) analyzed by *diskImageR* (Gerstein, et al. 2016) to measure the susceptibility/resistance (as the radius of the zone of inhibition (RAD_{20},)) and the tolerance (as the fraction of growth (FoG_{20},) in the zone of inhibition relative to growth outside it) for each strain. For most strains (69.2%), FoG_{20} levels were affected by temperature, with higher tolerance levels at 37˚C and 39°C than at 30˚C, and little difference between tolerance levels measured at 37°C vs 39°C (Fig. 1A). The susceptibility/resistance levels remained similar at the three temperatures. Thus, tolerance, but not resistance, was affected by both medium composition and temperature.

We classified the isolates into three groups based on the effect of temperature on growth temperature-dependence of the tolerance (FoG_{20} values): temperature-enhanced tolerant (**TET),** (non-tolerant at 30 ˚C but highly tolerant at higher temperatures (n=92, average FoG_{20} values of 0.21 ± 0.03, 0.63 ± 0.17, 0.68 ± 0.15, at 30˚C, 37˚C and 39˚C, respectively)); all-temperature tolerant (**ATT**), which had similar FoG_{20} values at all three temperatures (n=31, FoG_{20} values of 0.52 ± 0.12, 0.61 ± 0.15, 0.61 ± 0.15, at 30˚C, 37˚C and 39˚C, respectively); and non-tolerant (**NT**), which exhibited only baseline levels of FoG_{20} at all three temperatures (n=10, average FoG_{20} values 0.21 ± 0.03, 0.23 ± 0.03, 0.24 ± 0.03, at 30˚C, 37˚C and 39˚C, respectively). At 37˚C and 39˚C, 92.5% (123 out of 133) of the strains exhibited similar tolerance levels, while at 30˚C, 76.7% (102 out of 133) were not tolerant on the YPD medium (Fig. 1B). Thus, both body and febrile temperature promoted tolerance on YPD medium in most isolates.

Growth dynamics of tolerant cells are similar in a broad range of supra-MIC fluconazole concentrations

To better characterize the similarities and differences in the drug responses of the different classes of isolates, we used E-Test® strips to measure susceptibility as the MIC after 24 h of growth, and spot dilution assays (Xu, et al. 2021), analyzed at 48h, to measure tolerance. One representative isolate was used for each of the three temperature-response classes: SC5314 (the *C. albicans* lab strain) for TET, YJB-T1891, for ATT, and YJB-T490 for NT strain classes. The three isolates had the same MIC value (1 µg/ml) at 30˚C, 37˚C and 39˚C on YPD (Fig. 2A)). However, plating 10-fold dilutions in spot assays revealed significant differences in the ability of individual colonies to grow in the presence of FLC (Fig. 2B). For the TET isolate at 30°C, and for the NT isolates at all three temperatures, no growth was evident above the MIC, indicating that they were not tolerant under these conditions. By contrast, the isolates that exhibited tolerance (the ATT isolate at all three temperatures, and the TET isolate at 37˚C and 39˚C) grew similarly at all the drug concentrations tested (up to 128 µg/ml).

Thus, for TET and NT tolerant isolates, tolerant growth does not exhibit much concentration-dependence from 2-128 µg/ml FLC.

We investigated the impact of MIC and tolerance on population growth dynamics in the presence of FLC by plating 100-200 colony-forming units of each isolate on YPD plates supplemented with FLC at concentrations from 0.25-128 µg/ml. We monitored growth dynamics at both 30˚C and 37˚C for 48 h at 30 min intervals using *ScanLag*, which reports on the time of appearance and growth rates of individual colonies (Levin-Reisman, et al. 2014; Rosenberg, et al. 2018).

At 30°C, colonies from TET isolate SC5314 failed to grow at FLC concentrations above the MIC (1 µg/ml), while at 37°C, growth was detectable. Colonies of the ATT isolate (YJB-T1891) grew at both 30˚C and 37˚C in all FLC concentrations, regardless of the MIC (1 µg/ml) (Fig. 2C) and for the NT isolate (YJB-T490), no colonies grew at either 30˚C or 37˚C in the supra-MIC FLC concentrations. These results are consistent with those from the E-test and spot dilution assays above.

ScanLag also measures colony growth on agar and reports the time required for a colony to become detectable on the plate. This time of appearance (TOA) is considered a proxy of lag phase length (Levin-Reisman, et al. 2014). In all three strain types, at both 30˚C and 37˚C, the average colony TOA on drug plates was dose-independent at drug concentrations below the MIC. Above the MIC, the TOA of isolates that exhibited tolerance in the spot assays was longer than at sub-MIC drug concentrations, yet was dose-independent: the whole population appeared with a later TOA at all supra-MIC concentrations tested. In contrast to TOA, growth rate was dose-dependent at sub-MIC drug concentrations. Above the MIC, the growth rate, like the TOA, was slower than at sub-MIC concentrations, yet was drug dose independent. Thus, at supra-MIC drug concentrations, tolerant cells appeared later, presumably because they have a more prolonged lag phase, and grew slower than at sub-MIC concentrations. Nonetheless, these growth properties were similar at concentrations from 2 µg/ml to 128 µg/ml of fluconazole, consistent with the low degree of concentration-dependence of tolerance.

Evolution of higher tolerance from cells in the non-tolerant state

To ask how a non-tolerant isolate adapts to supra-MIC FLC concentrations, we plated approximately $1x10^6$ cells of TET isolate SC5314 and NT isolate YJB-T490 on YPD plates supplemented with 8 µg/ml to 128 µg/ml FLC. The plates were incubated under conditions where these isolates were non-tolerant: 30˚C for SC5314 and 30˚C and 37˚C for YJB-T490. As controls, we plated $1x10^6$ cells of SC5314 at 37°C and the ATT strain (YJB-T1891) at 30˚C and 37˚C on the same range of FLC concentrations. As expected, all controls produced a lawn of cells. By contrast, the TET strain at 30˚C and the NT strain at both temperatures gave rise to a few hundred to a few thousand colonies (adaptors) per plate after 5 days on the drug plates (Fig. S2).

Disk diffusion assays were then performed on 90 randomly selected adaptors from SC5314 and YJB-T490 parent strains (18 adaptors from each 30°C drug plate). All these adaptors had a notable increase of increased FoG_{20}, indicative of elevated tolerance (Fig. 3) when tested at 30°C. When tested at 37°C, all SC5314-derived adaptors (like the SC5314 ancestor) had high FoG_{20} (Fig. 3 Top panel), while all YJB-T490-derived adaptors had low FoG_{20} (Fig. 3 Middle panel). Thus, adaptors derived from SC5314 at 30˚C acquired tolerance at 30˚C and maintained their tolerance at 37˚C, and adaptors derived from YJB-T490 at 30˚C acquired tolerance that was limited to 30˚C. By contrast, many adaptors derived from YJB-T490 at 37˚C were tolerant at both 30˚C and 37˚C (Fig. 3 Bottom panel). Thus, depending on the temperature used to evolve the adaptors, the NT isolate adapted to FLC in two distinct manners: at 30°C they acquired a new type of conditional tolerance that we term *temperature-sensitive* tolerance (**TST)** seen only at 30°C and not at 37°C; when evolved at 37°C, NT isolates acquired tolerance that was detectable at both 30˚C and 37˚C, a phenotype akin to that of other ATT-like adaptors.

Recurrent aneuploidy enables the acquisition of fluconazole tolerance

To identify genomic mechanisms by which the SC5314 and YJB-T490-derived adaptors acquired tolerance, we performed deep sequencing of 18 independent adapted isolates for the TET and NT strains collected at 30˚C on 8 µg/ml, 32 µg/ml, and 128 µg/ml of fluconazole. Taken together, 54 adaptors derived at 30˚C from TET and NT isolates were sequenced.

Aneuploidy was prevalent among the adaptors. Out of the 54 TET-derived adaptors, one (FY9) that appeared on 8 µg/ml FLC plate grew poorly and was excluded from sequencing and further analysis. From the others, 50 (94.3%) were aneuploid (Fig. S3) and three were euploid. Among the 54 NT-derived adaptors at 30˚C, 52 (96.3%) were aneuploid (Fig. S4) and two were euploid. Four of the five euploid adapters (from TET- and NT-derived) appeared at 8 µg/ml FLC, the lowest selective drug concentration tested.

Analysis of the karyotypes revealed several recurrent aneuploidies, several of which were seen in both the TET- and NT-derived isolates. The most prevalent adaptors (35 TET adaptors; 27 NT adaptors) had aneuploidy involving ChrR, either as trisomy of the whole chromosome (ChrRx3) (9 from TET, 10 from NT), monosomy of the left arm distal to the rDNA repeats (SegChrRx1) (6 from TET), or trisomy of ChrR from rDNA repeats to the right telomere (SegChrRx3) (12 from NT), or a combination of SegChrRx3 and SegChrRx1 (10 from TET). These ChrR aneuploidies appeared alone or in combination with trisomy of other chromosome(s) (Chr4 or Chr7 in TET adaptors; any combination of Chr4 and Chr6 trisomy alone or together with trisomy of Chr7 in NT adaptors) (Fig. 4). Five TET adaptors and 19 NT adaptors had aneuploidy of chromosome(s) other than ChrR. The 5 TET adaptors had a single additional aneuploidy: SegChr1x1, Chr4x3, Chr4x4, SegChr5x1, or Chr6x3, (Fig. S3). Among the 19 NT adaptors, only one had a single aneuploid chromosome (Chr5x1) and this monosomic strain grew very slowly. The remaining 18 adaptors had at least two aneuploid chromosomes, mostly Chr4x3 together with Chr6x3 (Fig. S3 and summarized in Fig. 4).

Taken together, NGS revealed 21 different karyotypes among the 50 TET-derived ATT-like aneuploid adaptors, and 17 different karyotypes among the 53 NT-derived TST aneuploid adaptors. Despite differences in genetic background and FLC concentration used for selection, the same aneuploidies (predominantly ChrRx3 or SegChrRx3) were recurrently associated with the emergence of FLC tolerance. This occurred in both the ATT types derived from TET ancestral isolates and the TST types derived from NT ancestral isolates.

The NT-derived adaptors obtained at 37˚C also had diverse karyotypes. Each of the nine sequenced NT→ATT adaptors had a unique karyotype that was *not* seen in the NT→TST adaptors obtained at 30˚C (Fig. 4): 7 had amplification of Chr6 alone (n=1) or in combination with aneuploidy (mostly trisomy) of one or more other chromosomes (n=6). Only two NT→ATT adaptors did not have Chr6 aneuploidy: one adaptor had SegChr1x1 alone, and one had SegChr2x1 alone.

Taken together, the karyotypes of the adaptors were FLC dose-independent but temperature-dependent. At 30˚C, the TET- and NT-derived adaptor karyotypes involved recurrent ChrR amplification in TET→ATT and NT→TST adaptors selected across the range of FLC concentrations used. By contrast, from selection at 37°C, NT→ATT adaptors had distinctly different aneuploid adaptors: predominantly Chr6 trisomy and tetrasomy, alone or in combination with another aneuploid chromosome. Thus, selection at 30°C yielded similar karyotypes with different tolerance temperature responses in different strain backgrounds. Moreover, different selection temperature (30°C vs 37°C) yielded different karyotypes in the same strain background (NT→TST vs NT→ATT) (Fig. 3 and Fig. 4).

Loss of aneuploidy is associated with loss of acquired fluconazole tolerance.

Whole chromosome aneuploidies can be gained and lost through mitotic missegregation. Previously we found that reversible chromosome gain and loss affected general fitness and drug responses in *C. albicans* (Yang, et al. 2019; Yang, Todd, et al.

2021). Here, we asked if the FLC tolerance associated with recurrent aneuploidy was also unstable. Adaptors with different aneuploidies were spread onto YPD (without drug) and grown at 30˚C for 36h. All yielded a mixture of colony sizes, with primarily small (S) and some large (L) colonies (Fig. 5A), although the frequency of appearance of L colonies was different for different aneuploids. We randomly selected one S and one L colony from each strain and tested them by DDA at 30˚C.

To ask if point mutations had any role in the acquisition of tolerance, we performed variant calling to identify any SNPs of moderate to high effect (missense, nonsense, frameshift) that passed our qualify filters (see Materials and Methods) in the small (aneuploid) and large colonies of the tolerant adaptors (Table S1). Small and Large colonies from the same parent shared 14 SNPs. We assume that these SNPs were acquired during selection on fluconazole and were not drivers of tolerance. Taken together, in six tolerant adaptors representative of the six different karyotypes, we found variants that caused missense mutations in 23 genes. None of them were significantly (FDR > 0.1) enriched for gene ontology (GO) terms. Twelve genes were not annotated to any biological process, and 14 genes had unknown molecular functions. None of the SNPs found here were in genes encoding known or predicted drug efflux pumps or in known ergosterol biosynthesis enzymes or regulators.

Importantly, all the S colonies retained the higher tolerance seen in their parent strain and remained aneuploid like the adaptors from which they were derived. By contrast, all the L colonies were no longer tolerant (Fig. 5B) and had lost the aneuploid chromosome(s) to become euploid (Fig. 5C). This strong correlation, between the presence of aneuploidy and tolerance in all the S and loss of aneuploidy and tolerance in all the L progeny, supports the idea that the aneuploidies acquired during passaging on fluconazole were the major drivers of tolerance in the original adaptors. Because only some aneuploid chromosomes associated with tolerance, we presume that these aneuploidies appeared, in some cases recurrently, because they provide a selective advantage in the presence of drug (Janbon, et al. 1998; Selmecki, et al. 2008; Yang, et

al. 2013; Yang, et al. 2019; Yang, Gritsenko, Lu, et al. 2021; Yang, Gritsenko, Slor Futterman, et al. 2021).

Evolutionary trajectories differ at sub-MIC versus supra-MIC fluconazole concentrations

Because the TET and NT isolates acquired tolerance, but not resistance, when exposed to supra-MIC concentrations of FLC on solid medium, we next asked if this was a function of the FLC concentration. Therefore, we evolved one TET isolate (SC5314) and one NT isolate (YJB-T490) by passaging them daily (1:1000 dilutions) in YPD broth supplemented with FLC ranging from 4X below the MIC (0.25 µg/ml) to 128X above the MIC for a total of 15 days. As a control, we also passaged the isolates in YPD without drug.

Every five days an aliquot of each culture was washed, diluted, and ~ 200 cells were spread onto a YPD plate. In general, ~ 100 to 200 CFU appeared on the plates within 24h. We then randomly selected 18 or 96 colonies, from the TET and NT cultures, respectively. We always aimed to randomly select similar numbers of large, medium, and small colonies from each culture/drug concentration and tested their responses to FLC on disk diffusion assays. In total, we measured resistance (Rad_{20}) and tolerance (FoG_{20}) for 18 and 96 TET and NT derivatives per day of passage (1, 5, 10, and 15 days) and per drug concentration (0, 0.25, 0.5, 1, 2, 4, 8, 16, 32, 64 and 128 µg/ml fluconazole) for a total 792 (SC5314 derivatives) and 4224 (YJB-T490 derivatives) measurements, respectively (Fig 6A and 6B).

For SC5314 (MIC ~ 1µg/ml FLC), among the 504 adaptors evolved at supra-MIC concentrations (2-128 µg/ml FLC), most exhibited tolerance (increased FoG_{20}), while *none* of the adaptors acquired increased fluconazole resistance (Fig. 6A). In fact, some adaptors were *more susceptible* to fluconazole, as evidenced by a *larger* RAD_{20} (and thus a lower MIC_{20}) than the parent strain. Similarly, for YJB-T490 (MIC ~ 0.75-1 µg/ml), most of the 2688 adaptors evolved at supra-MIC concentrations (2-128 µg/ml), exhibited

tolerance, and *none* exhibited resistance (Fig. 6B). Interestingly, both the frequency with which tolerance arose and the range of tolerance levels achieved were similar at all the supra-MIC concentrations used for passaging (Fig. 6A). This suggests that once the drug inactivated its target, additional drug had little if any effect on how often or how much tolerance emerged.

At the MIC, SC5314 adaptors gained either resistance or tolerance (but not both) after 5 and 10 passages, while only resistant isolates appeared after 15 days of passaging at the MIC. Thus, it appears that at the MIC, SC5314 adaptors that were tolerant after 5 and 10 passages became resistant after 15 passages. Furthermore, there was stepwise increase in the level of resistance in adaptors evolved for 5, 10 and 15 days in 1 µg/ml FLC (Fig. 6A and Fig. S5). For YJB-T490 adaptors, only tolerant isolates were detected at the MIC. In some assays, the MIC of YJB-T490 is slightly lower than that of SC5314, and thus 1 µg/ml may be slightly higher than the actual MIC for this strain.

At sub-MIC concentrations (0.25 and 0.5 µg/ml), SC5314 adaptors became either resistant (decreased RAD_{20}) or tolerant (increased FoG_{20}) (but not both). Among the adaptors evolved in 0.25 µg/ml and 0.5µg/ml FLC, resistance emerged in 35 and 30 adaptors, respectively, while tolerance was detected in 1 and 6 adaptors, respectively. The remaining adaptors appear to have had more transient tolerance that had been lost during growth in the absence of FLC. Adaptors evolved for 10 and 15 days in 0.5 µg/ml FLC also exhibited stepwise increases in resistance. YJB-T490 adaptors also acquired either resistance or tolerance (but not both). Among adaptors evolved in 0.25 µg/ml FLC, tolerance appeared after ten passages; yet after 15 passages in 0.25 µg/ml FLC for 15 days, ten were tolerant, and 23 were resistant. At 0.5 µg/ml, the proportion of resistant YJB-T490 adaptors relative to tolerant adaptors increased over time (0 vs 58; 29 vs 18, and 72 vs 24, for adaptors from passages 5, 10 and 15, respectively (Fig. 6). While this is consistent with the idea that isolates may have acquired tolerance in early passages and then become resistant in the later passages, we cannot be sure that the resistant adaptors are progeny of the prior tolerant ones.

The dynamics of the emergence of tolerance and resistance also differed considerably. In both parental strain backgrounds tolerance emerged more rapidly, within a single passage, while the first resistant adaptors appeared after 5 passages and only in SC5314 at 1µg/ml FLC, while adaptors passaged in 0.25 µg/ml and 0.5 µg/ml only produced resistant and tolerant progeny after 10 days, and resistant adaptors after 15 days. In YJB-T490, *tolerant* adaptors evolved at or below the MIC 1 µg/ml, 0.5 µg/ml and 0.25 µg/ml initially appeared in passages 1, 5, and 10, respectively, while *resistant* adaptors that emerged from 0.5 µg/ml and 0.25 µg/ml FLC initially appeared on days 10 and 15, respectively. Thus, the acquisition of resistance and tolerance occurred at different relative stress levels (sub-MIC vs supra-MIC) and with different temporal dynamics (Fig. 6), and tolerant isolates generally appeared more rapidly than resistant isolates.

Distinct and diverse genetic alterations in fluconazole-resistant versus fluconazole-tolerant adaptors

Individual colonies that arose following the evolution of SC5314 in broth passages had a range of resistance or tolerance levels, suggesting that they may have acquired distinct genetic or genomic changes. To test this hypothesis, we sequenced 73 randomly selected adaptors (34 resistant and 39 tolerant) derived from SC5314. Large-scale genome changes were visualized with Ymap (Fig. 7 and Fig. S6), and variant calling was performed to identify mutations in predicted open reading frames, focusing on missense mutations and frameshift mutations.

Notably, all 39 tolerant adaptors that were sequenced were aneuploid (Fig. 7, lower section): 13 had whole or segmental aneuploidy only for all or segments of ChrR: (ChrRx3 (n=9), SegChrRx3 from 1.89Mb to right telomere (n=3), or SegChrRx1 from 1.89Mb to right telomere (n=1)). An additional 25 adaptors were aneuploid for ChrR in combination with aneuploidy of another one or two chromosomes (n=22 and n=3, respectively). Only one tolerant adaptor (Chr6x3, ABB, evolved over 10 passages in 1

µg/ml FLC) did not include copy number changes on ChrR. Thus, ChrR aneuploidy was the most prevalent aneuploidy associated with tolerance.

Among the 34 resistant adaptors sequenced, the majority (22/34) were euploid and 12 were aneuploid. Among the aneuploid adaptors, two (SY60 and SY61) had Chr3x3, five (SY20, SY21, SY22, SY51, SY55) had Chr5x3, four (SY50, SY56, SY58, SY59) had Chr7x3 (AAB), and one adaptor (SY57) had Chr6x3 (AAB) together with Chr7x3 (AAB). Notably, none of the resistant adaptors affected ChrR copy number and the karyotypes of the resistant adaptors were distinct from the tolerant adaptors (Fig. 7 and Fig.S5). Therefore, tolerant and resistant adaptors acquired distinct genomic changes: all tolerant adaptors were aneuploid, with ChrR aneuploidy as the predominant change while resistant adaptors were mostly euploid or were trisomic for either Chr3, Chr5, or Chr7.

Importantly, similar types of karyotypes were detected in SC5314 and YJB-T490 derived tolerant adaptors selected on supra-MIC FLC concentrations on agar plates (Fig. S3 and Fig. S4). Furthermore, the karyotypes of tolerant adaptors appeared in a dose-independent and time-independent manner (Table 1 and Fig. 7). For example, ChrRx3 aneuploidies appeared after one day in 2 µg/ml or 128 µg/ml FLC, after 5 days in 1 µg/m FLC, after 10 days in 0.25 µg/ml FLC, and after 15 days in 2 µg/ml FLC. Similarly, ChrRx3+Chr4x3 appeared after 1 day in 2 µg/ml FLC, 10 days in 1 µg/ml, 2 µg/ml and 128 µg/ml FLC, and after 15days in 2 µg/ml and 128 µg/ml FLC. And segChrRx3 (from the left telomere to 1.89 MB) appeared after 10 days in 0.5 µg/ml FLC, and 15 days in 2 µg/ml and 128 µg/ml FLC (Table 1). Thus, the same aneuploidies can arise at different concentrations and at different times after initial drug exposure.

To ask about point mutations that may influence the degree of tolerance or resistance, we identified SNPs in the 39 tolerant and 34 resistant adaptors (Table S2). In total we found from 2 to 5 SNPs per tolerant isolate and 0 to 2 SNPs per resistant isolate. One of the two ORFs with detectable SNPs in both a tolerant and a resistant adaptor was C2_08380C, a possible ortholog of *S. cerevisiae DPB11,* that, when mutated, causes

gross chromosomal rearrangements, chromosome loss and an increase in spontaneous DNA damage (Araki, et al. 1995). While the degree to which these specific SNPs affect the encoded function is not known, this gene might contribute to increased frequencies of mutations in the adaptors.

SNPs found only in *tolerant* adaptors were detected in 27 ORFs. However, of these 27 only one could be associated with drug tolerance: C1_04010C. We detected 2 SNPs in this ORF in 4 different adaptors. This gene encodes a protein with a predicted NADP-dependent oxidoreductase domain, and its transcript is induced by ketoconazole, yet is repressed by Upc2p, a transcription factor that up-regulates ergosterol biosynthesis (Synnott, et al. 2010). There was no statistically significant (FDR > 0.1) gene ontology term enrichment of these 27 genes. Thus, the few SNPs that appeared may be neutral mutations and do not appear to have any obvious connections to drug resistance or tolerance.

SNPs found only in *resistant* adaptors were detected in 7 genes with no detectable gene ontology term enrichment (FDR > 0.1), but none were in genes that encode efflux pumps, or that are known to affect ergosterol biosynthesis, the two major mechanisms of azole resistance. We suggest that some of these SNPs are probably neutral or nearly-neutral mutations that arose during the course of passaging and/or false positive variants that our quality filters were not stringent enough to filter out.

Discussion

Contrary to the concept from bacteria that antimicrobial drugs primarily select for the rapid evolution of drug resistance, here we found that *C. albicans*, a common cause of systemic bloodstream infections, primarily acquired tolerance to the widely used drug FLC. Importantly, this antifungal tolerance appeared rapidly, in some cases within a single day of exposure to drug concentrations above the strain MIC, while resistant isolates appeared after 5 days of exposure to low levels of FLC. Furthermore, the resistant isolates exhibited a stepwise increase in MIC levels (Fig. 6A), and we found no evidence that mutations in classic genes associated with FLC resistance played any role in the resistance acquired under the conditions used.

Here, we found that most clinical *C. albicans* isolates exhibit FLC tolerance at physiologically relevant temperatures, and not at 30°C, the temperature often used in lab studies (Fig. 1). This antifungal tolerance is largely dose-independent at supra-MIC drug concentrations (Fig. 2). Experimental evolution in supra-MIC drug concentrations rapidly selected for the acquisition of tolerance that was associated with a recurrent set of aneuploidies (Figs. 3,4,6,7). Resistant isolates only appeared at or below the MIC, after 5 or more days of passaging (Fig. 6). While most resistant isolates were not aneuploid, those that carried recurrent aneuploidies had extra copies of different chromosomes from those seen in tolerant isolates (Fig. 7). Furthermore, resistance (but not tolerance) appeared to be acquired in a stepwise manner (Fig. 6). Thus, experimental evolution at sub-MIC FLC concentrations selected for isolates that were either only tolerant or only resistant, and a different set of recurrent aneuploidies conferred tolerance vs resistance.

Of the original 133 clinical *C. albicans* isolates tested at 37°C and 39°C, up to 92.5% of the isolates were tolerant, while at 30°C only 23.3% of isolates were tolerant. Thus, it appears that FLC tolerance is prevalent in clinical isolates, at least those collected from Israeli patients. These clinical strains are largely euploid; thus, we suggest that tolerance is primarily due to genomic factors, including inherent genetic backgrounds,

that modulate stress responses in different physiological conditions, such as temperature and medium composition. In addition, the acquisition of aneuploidy can increase or modulate tolerance levels. While this study focused on 133 Israeli clinical isolates, it will be interesting to determine if other clinical isolates exhibit temperature-enhanced tolerance.

Tolerant isolates were able to grow at supra-MIC fluconazole concentrations up to 128 µg/ml. Furthermore, the time of colony appearance, as well as growth rate of colonies on drug plates were dose-independent at supra-MIC FLC concentrations. Yet, below the MIC, colony growth rates were dose-dependent with colonies growing more slowly with increasing drug concentrations. This suggests that *C. albicans* mounts distinct cellular responses at sub-MIC versus supra-MIC drug concentrations. The concentration-independent nature of tolerant cell growth rates and the initial time of colony appearance at supra-MIC, and the concentration-dependent nature of resistance (Fig. 2B and C) at sub-MIC concentrations, highlights probably mechanistic differences between these processes. We posit that tolerance involves cellular stress mechanisms that are less sensitive to the intracellular drug concentration and enable growth when the drug target, in this case lanosterol demethylase, is completely inactivated by drug. The fact that different aneuploidies or mutations accompany tolerance vs resistance further supports this idea. Furthermore, isolates with different genetic backgrounds at the temperatures used and on agar or in broth media, adapted to supra-MIC FLC primarily by acquiring the same aneuploidies involving ChrR.

All tolerant adaptors had at least one aneuploid chromosome. In addition to the recurrent karyotypes involving ChrR aneuploidies, some tolerant adaptors acquired other aneuploidies. This suggests that individual cells use a similar strategy, chromosome instability, to reach non-identical outcomes (e.g., different levels of acquired tolerance) from different combinations of aneuploid chromosomes that provide a growth advantage in supra-MIC drug concentrations. Even though we detected a few SNPs in the aneuploid isolates and we do not know the degree to which they may (or may not) contribute to tolerance, the fact that loss of the aneuploid chromosome(s) was

accompanied by loss of FLC tolerance suggests that aneuploidy was the primary mechanism conferring tolerance.

Strain background and environmental conditions also contribute to the selective conditions that favor the acquisition of different aneuploidies. Interestingly, in both the TET and NT backgrounds, amplification of portions of ChrR enabled tolerance at 30˚C but not at 37˚C. Yet, for the NT strain, Chr6 trisomy increased tolerance at both 30˚C and 37˚C in the presence of the same range of FLC concentrations. Thus, the rapid emergence of tolerance can occur via multiple routes, and the trajectories of the routes are affected by the original strain background and the selection conditions. Future work will require analyzing the trajectories of adaptation of additional TET and NT isolates and identifying the chromosomal region(s) that specifically affect tolerance at different temperatures.

Some of the tolerant adaptors also became less FLC resistant (more susceptible, larger RAD_{20},). This was also seen for isolates passaged in posaconazole, another fungistatic azole (Kukurudz, et al. 2022). This supports the idea that the acquisition of antifungal resistance and antifungal tolerance follow different trajectories and that supra-MIC concentrations preferentially and can rapidly select for azole tolerance along with decreased azole resistance.

All tolerant strains acquired aneuploidy together and had a similar range of tolerance levels at all supra-MIC concentrations. By contrast, the resistant mutations that appeared at concentrations at or below the MIC, continued to become more resistant over time (Fig. 6 and Fig. S5). Interestingly, this stepwise acquisition of improved fitness was seen both with aneuploid and euploid resistant adaptors. This highlights the very different evolutionary trajectories that occur above and below the MIC. At all the supra-MIC concentrations tested, when the drug target is completely inhibited/saturated by drug, cells must respond with strategies independent of the drug-target interaction. By contrast, at sub-MIC concentrations, the drug target is not saturated, all cells are able to grow to some degree, providing the opportunity for the acquisition of a series of

mutations that incrementally increased resistance. At sub-MIC, tolerance also emerged occasionally.

Why does aneuploidy appear so rapidly and with such a high frequency (~10^{-3}) following exposure to supra-MIC drug concentrations? We suggest that three forces drive the rapid appearance of aneuploidy at high frequency: first, random aneuploid chromosomes maintained in the parent population may provide standing variation; second, fluconazole induces chromosome mis-segregation via cell cycle defects that yield tetraploid intermediates and, subsequently, random aneuploids (Harrison, et al. 2014; Altamirano, et al. 2017) at high frequency; and third, strong selection for specific aneuploidies that provide an adaptive advantage in the presence of the drug allows the aneuploid isolates to compete and outgrow arrested euploid cells (Yang, Todd, et al. 2021). Chromosome mis-segregation events that lead to whole chromosome aneuploidy are relatively frequent (every 5x10^5 cell divisions in yeast (Hartwell, et al. 1982) and on the order of once every 10^4 to 10^5 divisions in mammalian cells (Rosenstraus and Chasin 1978)). Since *C. albicans* chromosomes contain between 407-1383 genes per chromosome (http://www.candidagenome.org/cache/C_albicans_SC5314_genomeSnapshot.html, as of Nov 24, 2022), it follows that a single aneuploid chromosome should affect the stoichiometry of many proteins. Even if these aneuploidies have a fitness cost under standard growth conditions, if they provide a fitness advantage in drug, they should be maintained at least until classic point mutations, with better fitness are selected and ultimately out-compete the aneuploids (Yona, et al. 2012). Segmental aneuploidies, which are dependent upon recombination events, also appeared. It is tempting to speculate that either drug stress increases the likelihood of mitotic recombination as was seen for LOH events (Forche, et al. 2011), or that recombination events are more frequent in strains carrying aneuploid chromosomes. Consistent with this idea, haploid *S. cerevisiae* lab strains carrying single extra chromosomes conferred increased mitotic recombination as well as chromosome instability (Sheltzer, et al. 2011).

In this study, tolerant adaptors emerged more rapidly (within one passage) than resistant adaptors. Ultimately, all supra-MIC isolates became tolerant, while only some of the sub-MIC adapters became resistant. Indeed, even resistant adaptors that had acquired resistance via aneuploidy appeared much later in the passaging and appear to have arisen from tolerant intermediates (e.g., some adaptors evolved in 0.5 µg/ml and 1 µg/ml FLC were tolerant on day 10, but all were resistant on day 15, and some were aneuploid (Fig. 6)). Thus, while the dynamics of acquiring tolerance is different at sub- and supra-MIC drug concentrations, a similar set of aneuploidies confers resistance, and a different set of aneuploidies can confer tolerance.

In *C. albicans*, two major mechanisms contribute to FLC resistance: alteration of the drug target and increased drug efflux. A combination of these mechanisms causes stepwise development of FLC resistance ((Sasse, et al. 2012); reviewed in (Morschhauser 2002)) or can arise in a single segmental aneuploidy (Selmecki, et al. 2008). Surprisingly, we did not find any of the classic resistance mutations in resistant adaptors. This could be due to the high fitness cost of mutations in these genes (Sasse, et al. 2012; Hill, et al. 2015; Popp, et al. 2017). In the presence of sub-MIC FLC, cells are under weak stress and mutations with a high fitness cost might be outcompeted. In general, gain-of-function mutations in *MRR1*, *TAC*, or *UPC2* in FLC-resistant clinical isolates incur a fitness cost and are outcompeted by the matched susceptible isolates both *in vitro* and in *vivo* (Popp, et al. 2017). Artificially introducing resistance-enhancing mutations causes a stepwise increase in resistance that is associated with a gradual reduction in fitness both in *vivo* and *in vitro* (Sasse, et al. 2012). Similarly, experimental evolution with increasing amounts of FLC yielded resistant mutants with mutations in *TAC1*, *UPC2,* and/or *ERG11* that were less fit than their parents in macrophages, as well as in the presence of several stresses, including cell wall stress, cell membrane stress, salt stress, oxidative stress and temperature stress (Hill, et al. 2015). The longer time required for resistant adaptors to arise, even if aneuploid, provides indirect support for the idea that resistance is due to the accumulation of multiple mutational events.

Cells appear to adopt different adaptive trajectories at supra-MIC versus sub-MIC drug concentrations. At supra-MIC FLC, extreme stress may favor the immediate appearance of tolerance, perhaps because aneuploidy can appear within a single cell division or because aneuploidy may slow growth and thus might slow drug metabolism. At sub-MIC FLC concentrations, cells experience only mild stress that does not affect cell survival, which may enable the evolution of resistance in a stepwise manner. The degree of resistance, measured by the MIC or RAD, can increase over time of exposure to the drug (Fig. 6 and Fig. S5). Accordingly, more extended passaging at sub-MIC FLC concentrations yields adaptors with higher MIC levels. We speculate that this may involve a sequential acquisition of several different types of resistance mutations, including point mutations that confer stable drug resistance.

In bacteria, both sub- and supra-MIC antibiotic concentrations select for resistant mutants, but different selection strengths confer different evolutionary trajectories and drive the acquisition of different mutations. When selected in cidal antibiotics at supra-MIC drug concentrations, resistance mutations in one or a small number of “classical” resistance genes are selected. But when exposed to low antibiotic concentrations, bacteria accumulate mutations of several “non-classic” genes that individually confer weak resistance but together can confer higher resistance levels (Wistrand-Yuen, et al. 2018). In addition, selection at sub-MIC antibiotic concentrations can select for plasmids carrying multiple resistance genes that lead to multidrug resistance (MDR) (Gullberg, et al. 2014).

In summary, FLC tolerance is prevalent in *C. albicans* clinical isolates, especially at 37°C and it exhibits different temperature responses in different strain backgrounds. The acquisition of resistance and tolerance occurs via distinct evolutionary trajectories that are largely a function FLC stress levels: supra-MIC FLC stress drives tolerance, which appears rapidly and enables growth at wide range of supra-MIC drug concentrations; sub-MIC FLC stress selects for either tolerance or stepwise elevated resistance. Different strains have different intrinsic levels of tolerance, but they generally appear to rapidly acquire additional tolerance by becoming trisomic for specific

chromosomes. The most commonly acquired aneuploidy in tolerant adaptors is part or all of ChrR, while trisomy of Chr3 or Chr5, are associated with the relatively rapid appearance of increased antifungal drug resistance.

Materials and Methods

Strains and growth conditions

Strains use in this study are listed in Table S3. Stock cultures of all strains were preserved in 35% glycerol and maintained at -80°C. The 133 clinical *C. albicans* were collected from hospitals in Israel and kindly provided by Ronen Ben-Ami. Unless otherwise specified, cells were routinely grown on Yeast extract-Peptone-Dextrose (YPD)-agar media (1% [w/v] yeast extract, 2% [w/v] peptone and 2% [w/v] D-glucose, 2%[w/v] agar) at 30°C. Other media used in this study include casitone agar plates (0.9%[wt/vol] casitone, 0.5% [wt/vol] yeast extract, 1.15% sodium citrate dihydrate [wt/vol], 2% [wt/vol] glucose, 2% [wt/vol] d-glucose, and 2% [wt/vol] agar), SD agar plates (0.67% [wt/vol] yeast nitrogen base without amino acids, 2% [wt/vol] d-glucose, and 2% [wt/vol] agar), and SDC agar plates (0.67% [wt/vol] yeast nitrogen base without amino acids, 2% [wt/vol] d-glucose, 0.2% [wt/vol] complete amino acid mixture, and 2% [wt/vol] agar). Drugs were dissolved in dimethyl sulfoxide (DMSO) and stored at -20°C.

E-test strip assays

E-tests were performed as described previously (Yang, Gritsenko, Lu, et al. 2021). Strains were streaked from -80˚C freezer onto YPD agar. After incubation at designated temperature (30, 37 or 39°C) for 24h, colonies were chosen randomly and suspended in distilled water. Cell density was determined using a hemocytometer. Cells were adjusted to $1x10^6$ cells/ml, and 100 µl of the culture was spread on YPD agar. The plate with an FLC E-test strip (BioMerieux, Marcy l'Etoile, France) at the center was incubated at designated temperature for 24h and then photographed.

Disk diffusion assays

Disk diffusion assays were performed as previously described (Rosenberg, et al. 2018; Xu, et al. 2021). The CLSI M44-A2 guidelines for antifungal disk diffusion susceptibility testing were followed with slight modifications. Briefly, strains were streaked from glycerol stocks onto YPD agar and incubated for 36h at designated temperatures. Colonies were suspended in distilled water and adjusted to $1x10^6$ cells/ml. 100 µl of cell suspension were spread onto 15 ml YPD plates. An empty paper disk (6 mm diameter, and 0.7 mm thickness) supplemented with 5 µl of 5 mg/ml FLC was placed in the center of each plate. Plates were then incubated at designated temperature and photographed at 24h and 48h. Analysis of the disk diffusion assay was done using the *diskImageR* pipeline (Gerstein, et al. 2016). The fraction of growth inside the zone of inhibition and radius of inhibition, referred to as FoG and RAD throughout the manuscript, represent parameters measured at 20% drug inhibition (FoG_{20} and RAD_{20}, respectively).

Spot assay

Cells were suspended in distilled water and counted using a hemocytometer. Cell density was adjusted to $1x10^7$ cells/ml. 3 µl of 10-fold serial dilutions were spotted on YPD plates with or without drugs (control). The plates were incubated at the designated temperature and photographed after 2 days.

ScanLag assay

The *ScanLag* assay was performed as described in (Rosenberg, et al. 2018) with minor modifications. Approximately 100 cells were spread onto YPD plates with or without FLC. The plates were placed on the scanners at designated temperature and scanned every 30 min for 48 h. Image analysis was done in MATLAB using the modified "ScanLag" script (Levin-Reisman, et al. 2014; Rosenberg, et al. 2018).

Obtaining drug adaptors from plates

Cells were adjusted to $1x10^7$ cells/ml as described above. 100 µl of the culture were spread on YPD plates supplemented with drugs. The plates were incubated at the designated temperature for 5 days. Adaptors were randomly chosen.

Daily passage in YPD broth supplemented with fluconazole

SC5314 was inoculated into 1ml YPD broth at a final density of approximately $2.5x10^3$ cells/ml. The YPD broth was supplemented with DMSO (negative control) or with 2-fold increase of FLC from 0.25 µg/ml – 128 µg/ml FLC. Every 24h or when the OD600 of culture was higher than 1.0, 1 µl of each culture was inoculated into 1ml YPD broth supplemented with the same concentration of FLC. After 1, 5, 10, and 15 days, the 200 µl cultures were washed and diluted with distilled water. Approximately 100 cells were spread on YPD plates. The plates were incubated at 30°C for 36 h and 18 colonies from each plate were randomly tested with DDAs using FLC-containing disks.

Colony instability assay

As described previously (Yang, Todd, et al. 2021), aneuploid strains were streaked from -80˚C freezer to YPD plates and incubated at 30˚C for 36 h. One small colony was randomly chosen and suspended in distilled water. Cells were diluted with distilled water and approximately 200 cells were spread on a YPD plate and incubated at 30˚C for 36 h. One small (S) colony and one large (L) colony were randomly chosen for further studies.

Next generation sequencing (NGS)

NGS was performed as described in (Yang, Todd, et al. 2021).

Variant calling

Paired-end short reads of all sequences obtained from NGS were trimmed with Trimmomatic (version 0.39; (Bolger, et al. 2014)) with default settings and read quality. Trimmed reads were aligned to both alleles of the *C. albicans* reference genome

(GCF_000182965.3_ASM18296v3) with Burrows-Wheeler Aligner (bwa mem, version 0.7.17; (Li and Durbin 2009)). The alignments were sorted with SAMtools (samtools view; samtools sort; version 1.15.1; (Li, et al. 2009)), and duplicates were marked and removed with Picard Tools (version 2.27.5; available at http://broadinstitute.github.io/picard/). Indels were then realigned with GATK (version 3.8-1-0; (Auwera and O'Connor 2020)), and the alignments were resorted and reindexed with SAMtools. Variants (SNPs and indels) were called using FreeBayes (-J -K --report-genotype-likelihood-max -a -F 0.1; version 0.9.21; (Garrison and Marth 2012)). Variants that were present in both ancestor and evolved strains were removed using BCFtools (isec; version 1.16-17; (Li, et al. 2009)), filtered for quality with BCFtools, and annotated with SNPeff (version 5.1d; (Cingolani, et al. 2012)). The validity of each high-quality variant was then checked using the Integrative Genomics Viewer (IGV; version 2.15.1; (Robinson, et al. 2011))

GO analysis

Gene Ontology Term Finder tool on Candida Genome Database (http://www.candidagenome.org/cgi-bin/GO/goTermFinder) was used for functional enrichment analysis**,** using default parameters. Only hits with p-value corrected for false positives FDR < 0.1 were considered as significant.

Data availability

All sequence data are available in the ArrayExpress database at EMBL-EBI (www.ebi.ac.uk/arrayexpress) under accession numbers E-MTAB-12175, E-MTAB-12155, E-MTAB-12169 and E-MTAB-12189.

Acknowledgements

We thank Jacob Steenwyk for helpful suggestions. This work was supported by the National Key Research and Development Program of China (2021YFC2300400), the National Natural Science Foundation of China (NO. 82020108032), and the Innovation Program of Shanghai Municipal Education Commission (NO. 202101070007E00094) to

Yuan-ying Jiang. National Natural Science Foundation of China (NO. 81872910), and Shanghai Key Basic Research Project (NO. 19JC1414900) to Yong-bing Cao. Judith Berman also received funding from the European Research Council (ERC) under the European Union's Horizon 2020 research and innovation programme (grant agreement No 951475).

Figure legends

Figure 1. Measuring tolerance levels at 30˚C, 37˚C, and 39˚C identify three classes temperature response.

Disk diffusion assays were performed on 133 different clinical isolates at the indicated temperatures (30˚C, 37˚C, and 39˚C). The isolates were classified as temperature-enhanced tolerant (TET), all-temperature tolerant (ATT), and non-tolerant (NT), based on FoG_{20} values at the three temperatures. ** indicates p-value<0.001 as determined by two-tailed paired t-test (**A)**. **B** is the distribution of tolerant isolates at different temperatures (n=133). At 30 ˚C, 69.2% were TET, 23.3% ATT, 7.5% NT. Thus, the vast majority of strains exhibit tolerance at least at some temperatures.

Figure 2. Temperature dependent growth dynamics of representative TET, ATT and NT strains in different drug concentrations.

Representative isolates (TET, SC5314; ATT, YJB-T1891; and NT, YJB-T490) were assayed on plates with FLC E-Test strips (A) and on 10-fold dilution spot assays (B) at 30˚C, 37˚C and 39˚C on YPD medium at the FLC concentrations indicated. In both cases, plates were photographed after 48h at the indicated temperatures. Growth dynamics of isolates in the presence of FLC were measured using *ScanLag* (Levin-Reisman, et al. 2014; Rosenberg, et al. 2018). Approximately 100 colonies of the test strains were plated onto YPD plates supplemented with FLC at the concentrations indicated (C). The growth of colonies was monitored at 30˚C and 37˚C using *ScanLag*. Colony area was calculated from the area of light pixels in the images, a proxy for colony size, and the change in colony size over time was used to estimate colony growth rate. Note in (B) and (C), for tolerant isolates, growth was similar at all

817 fluconazole concentrations equivalent to and above MIC. The graphs show the
818 distribution of Time of colony Appearance (TOA, top panel) and growth rate (bottom
819 panel) for all colonies on each plate, in 72 hours (top panel). The area of colonies
820 occupied by light pixels and the change in this area over time are proxies for colony size
821 and growth rate.
822
823 **Figure 3. Selection for adaptors at supra-MIC fluconazole concentrations.**
824 FLC adaptors derived from TET strain SC5314 at 30˚C, and those derived from the NT
825 strain YJB-T490 at 30˚C and 37˚C, were tested for resistance (RAD_{20}) and tolerance
826 (Fog_{20}) on disk diffusion assays at 30˚C and 37˚C. The disks contained 25 µg FLC. The
827 plates were photographed at 24h and 48h for measuring RAD_{20} and FoG_{20}, respectively.
828 Each plot represents the data from 18 colonies that adapted to fluconazole
829 concentrations indicated in YPD plates. In the parents, 16 individual colonies were
830 tested.
831
832 **Figure 4. Recurrent aneuploidies associated with resistant and tolerant**
833 **fluconazole adaptors**
834 (A) Karyotypes recurrently identified in TET and NT derived fluconazole adaptors
835 selected at 30˚C. The total number of aneuploid adaptors, and the number of adaptors
836 bearing each karyotype are also indicated. Chromosomes 1,2,3,5, which were euploid
837 in these karyotypes, are not shown. (B) Karyotypes of 9 adaptors derived from NT
838 isolate at 37˚C. None of the karyotypes was identified in (A). The grey colored
839 karyotypes include adaptors with aneuploidy of different homologs of the same
840 chromosomes. The detailed karyotypes are shown in Fig. S3 and Fig. S4.
841
842 **Figure 5. Tolerance acquisition and loss is associated with the gain and loss of**
843 **aneuploid chromosomes**
844 Strains with different aneuploid chromosomes were spread onto YPD plates and grown
845 for 36 h at 30˚C. Small colonies (S) and large colonies (L), indicated by yellow arrows
846 and cyan arrows, respectively (A) were tested by standard disc diffusion assays (25 µg

FLC per disk). The plates were incubated at 30˚C for 48 h (B). Both S and L colonies were sequenced. The karyotypes were visualized by using Ymap (C).

Figure 6. Distinct evolutionary trajectories associated with supra- and sub-MIC fluconazole concentrations.

Emergence of tolerance (increased FoG_{20}) and resistance (decreased RAD_{20}) measured on disk diffusion assays for 18 isolates from each indicated passage of TET isolate SC5314 (A) and NT isolate YJB-T490 (B) for 1-15 days of propagation at the indicated drug concentrations. The MIC (1µg/ml) is highlighted in grey. Note that a broad range of tolerance emerges at all supra-MIC concentrations starting at passage 1, while increasing levels of resistance appear with time at or below the MIC only.

Figure 7. Distinct genomic changes in resistant and tolerant adaptors.

DNA sequences of 34 FLC-resistant and 39 FLC-tolerant adaptors evolved from TET strain SC5314 were analyzed by Ymap (Abbey, et al. 2014). The karyotypes, number of adaptors with this karyotype. and the drug conditions (number of days evolved and FLC concentration) are indicated to the right of each karyotype diagram. For example, D5-1 indicates that the adaptors were evolved for 5 days in 1 µg/ml FLC. Colors indicate allele frequencies in the data as indicated in the key. Black histograms indicate the log1 ratio of DNA copy number for the strain indicated relative to a diploid control

Table 1. Karyotypes of the 34 resistant and 39 tolerant evolved progeny analyzed.

References

Abbey DA, Funt J, Lurie-Weinberger MN, Thompson DA, Regev A, Myers CL, Berman J. 2014. YMAP: a pipeline for visualization of copy number variation and loss of heterozygosity in eukaryotic pathogens. Genome Med 6:100.

Altamirano S, Fang D, Simmons C, Sridhar S, Wu P, Sanyal K, Kozubowski L. 2017. Fluconazole-Induced Ploidy Change in Cryptococcus neoformans Results from the Uncoupling of Cell Growth and Nuclear Division. mSphere 2.

Araki H, Leem SH, Phongdara A, Sugino A. 1995. Dpb11, which interacts with DNA polymerase II(epsilon) in Saccharomyces cerevisiae, has a dual role in S-phase progression and at a cell cycle checkpoint. Proc Natl Acad Sci U S A 92:11791-11795.

Auwera GVd, O'Connor B. 2020. Genomics in the Cloud: Using Docker, GATK, and WDL in Terra. In: O'Reilly Media.

Berman J, Krysan DJ. 2020. Drug resistance and tolerance in fungi. Nat Rev Microbiol 18:319-331.

Bolger AM, Lohse M, Usadel B. 2014. Trimmomatic: a flexible trimmer for Illumina sequence data. Bioinformatics 30:2114-2120.

Bongomin F, Gago S, Oladele RO, Denning DW. 2017. Global and Multi-National Prevalence of Fungal Diseases-Estimate Precision. J Fungi (Basel) 3.

Carolus H, Pierson S, Lagrou K, Van Dijck P. 2020. Amphotericin B and Other Polyenes-Discovery, Clinical Use, Mode of Action and Drug Resistance. J Fungi (Basel) 6.

Cingolani P, Platts A, Wang le L, Coon M, Nguyen T, Wang L, Land SJ, Lu X, Ruden DM. 2012. A program for annotating and predicting the effects of single nucleotide polymorphisms, SnpEff: SNPs in the genome of Drosophila melanogaster strain w1118; iso-2; iso-3. Fly (Austin) 6:80-92.

Enoch DA, Yang H, Aliyu SH, Micallef C. 2017. The Changing Epidemiology of Invasive Fungal Infections. Methods Mol Biol 1508:17-65.

Fisher MC, Alastruey-Izquierdo A, Berman J, Bicanic T, Bignell EM, Bowyer P, Bromley M, Bruggemann R, Garber G, Cornely OA, et al. 2022. Tackling the emerging threat of antifungal resistance to human health. Nat Rev Microbiol 20:557-571.

Forche A, Abbey D, Pisithkul T, Weinzierl MA, Ringstrom T, Bruck D, Petersen K, Berman J. 2011. Stress alters rates and types of loss of heterozygosity in Candida albicans. mBio 2.

Garrison EP, Marth GT. 2012. Haplotype-based variant detection from short-read sequencing. arXiv: Genomics.

Gerstein AC, Rosenberg A, Hecht I, Berman J. 2016. diskImageR: quantification of resistance and tolerance to antimicrobial drugs using disk diffusion assays. Microbiology (Reading) 162:1059-1068.

Gullberg E, Albrecht LM, Karlsson C, Sandegren L, Andersson DI. 2014. Selection of a multidrug resistance plasmid by sublethal levels of antibiotics and heavy metals. mBio 5:e01918-01914.

Harrison BD, Hashemi J, Bibi M, Pulver R, Bavli D, Nahmias Y, Wellington M, Sapiro G, Berman J. 2014. A tetraploid intermediate precedes aneuploid formation in yeasts exposed to fluconazole. PLoS Biol 12:e1001815.

Hartwell LH, Dutcher SK, Wood JS, Garvik B. 1982. The fidelity of mitotic chromosome reproduction in S. cerevisiae. Rec Adv Yeast Mol Biol 1:28-38.

912 Hill JA, O'Meara TR, Cowen LE. 2015. Fitness Trade-Offs Associated with the Evolution of
913 Resistance to Antifungal Drug Combinations. Cell Rep 10:809-819.
914 Janbon G, Sherman F, Rustchenko E. 1998. Monosomy of a specific chromosome determines L-
915 sorbose utilization: a novel regulatory mechanism in Candida albicans. Proc Natl Acad Sci U S A
916 95:5150-5155.
917 Kukurudz RJ, Chapel M, Wonitowy Q, Adamu Bukari AR, Sidney B, Sierhuis R, Gerstein AC. 2022.
918 Acquisition of cross-azole tolerance and aneuploidy in Candida albicans strains evolved to
919 posaconazole. G3 (Bethesda) 12.
920 Levin-Reisman I, Fridman O, Balaban NQ. 2014. ScanLag: high-throughput quantification of
921 colony growth and lag time. J Vis Exp.
922 Levinson T, Dahan A, Novikov A, Paran Y, Berman J, Ben-Ami R. 2021. Impact of tolerance to
923 fluconazole on treatment response in Candida albicans bloodstream infection. Mycoses 64:78-
924 85.
925 Li H, Durbin R. 2009. Fast and accurate short read alignment with Burrows-Wheeler transform.
926 Bioinformatics 25:1754-1760.
927 Li H, Handsaker B, Wysoker A, Fennell T, Ruan J, Homer N, Marth G, Abecasis G, Durbin R,
928 Genome Project Data Processing S. 2009. The Sequence Alignment/Map format and SAMtools.
929 Bioinformatics 25:2078-2079.
930 Morschhauser J. 2002. The genetic basis of fluconazole resistance development in Candida
931 albicans. Biochim Biophys Acta 1587:240-248.
932 Pappas PG, Kauffman CA, Andes DR, Clancy CJ, Marr KA, Ostrosky-Zeichner L, Reboli AC,
933 Schuster MG, Vazquez JA, Walsh TJ, et al. 2016. Clinical Practice Guideline for the Management
934 of Candidiasis: 2016 Update by the Infectious Diseases Society of America. Clin Infect Dis 62:e1-
935 50.
936 Pfaller MA, Diekema DJ, Turnidge JD, Castanheira M, Jones RN. 2019. Twenty Years of the
937 SENTRY Antifungal Surveillance Program: Results for Candida Species From 1997-2016. Open
938 Forum Infect Dis 6:S79-S94.
939 Popp C, Hampe IAI, Hertlein T, Ohlsen K, Rogers PD, Morschhauser J. 2017. Competitive Fitness
940 of Fluconazole-Resistant Clinical Candida albicans Strains. Antimicrob Agents Chemother 61.
941 Robbins N, Caplan T, Cowen LE. 2017. Molecular Evolution of Antifungal Drug Resistance. Annu
942 Rev Microbiol 71:753-775.
943 Robbins N, Wright GD, Cowen LE. 2016. Antifungal Drugs: The Current Armamentarium and
944 Development of New Agents. Microbiol Spectr 4.
945 Robinson JT, Thorvaldsdottir H, Winckler W, Guttman M, Lander ES, Getz G, Mesirov JP. 2011.
946 Integrative genomics viewer. Nat Biotechnol 29:24-26.
947 Roemer T, Krysan DJ. 2014. Antifungal drug development: challenges, unmet clinical needs, and
948 new approaches. Cold Spring Harb Perspect Med 4.
949 Rosenberg A, Ene IV, Bibi M, Zakin S, Segal ES, Ziv N, Dahan AM, Colombo AL, Bennett RJ,
950 Berman J. 2018. Antifungal tolerance is a subpopulation effect distinct from resistance and is
951 associated with persistent candidemia. Nat Commun 9:2470.
952 Rosenstraus MJ, Chasin LA. 1978. Separation of linked markers in Chinese hamster cell hybrids:
953 mitotic recombination is not involved. Genetics 90:735-760.

954 Sasse C, Dunkel N, Schafer T, Schneider S, Dierolf F, Ohlsen K, Morschhauser J. 2012. The
955 stepwise acquisition of fluconazole resistance mutations causes a gradual loss of fitness in
956 Candida albicans. Mol Microbiol 86:539-556.
957 Selmecki A, Gerami-Nejad M, Paulson C, Forche A, Berman J. 2008. An isochromosome confers
958 drug resistance in vivo by amplification of two genes, ERG11 and TAC1. Mol Microbiol 68:624-
959 641.
960 Sheltzer JM, Blank HM, Pfau SJ, Tange Y, George BM, Humpton TJ, Brito IL, Hiraoka Y, Niwa O,
961 Amon A. 2011. Aneuploidy drives genomic instability in yeast. Science 333:1026-1030.
962 Synnott JM, Guida A, Mulhern-Haughey S, Higgins DG, Butler G. 2010. Regulation of the hypoxic
963 response in Candida albicans. Eukaryot Cell 9:1734-1746.
964 Wistrand-Yuen E, Knopp M, Hjort K, Koskiniemi S, Berg OG, Andersson DI. 2018. Evolution of
965 high-level resistance during low-level antibiotic exposure. Nat Commun 9:1599.
966 Xu Y, Lu H, Zhu S, Li WQ, Jiang YY, Berman J, Yang F. 2021. Multifactorial Mechanisms of
967 Tolerance to Ketoconazole in Candida albicans. Microbiol Spectr 9:e0032121.
968 Yang F, Gritsenko V, Lu H, Zhen C, Gao L, Berman J, Jiang YY. 2021. Adaptation to Fluconazole
969 via Aneuploidy Enables Cross-Adaptation to Amphotericin B and Flucytosine in Cryptococcus
970 neoformans. Microbiol Spectr 9:e0072321.
971 Yang F, Gritsenko V, Slor Futterman Y, Gao L, Zhen C, Lu H, Jiang YY, Berman J. 2021.
972 Tunicamycin Potentiates Antifungal Drug Tolerance via Aneuploidy in Candida albicans. mBio
973 12:e0227221.
974 Yang F, Kravets A, Bethlendy G, Welle S, Rustchenko E. 2013. Chromosome 5 monosomy of
975 Candida albicans controls susceptibility to various toxic agents, including major antifungals.
976 Antimicrob Agents Chemother 57:5026-5036.
977 Yang F, Teoh F, Tan ASM, Cao Y, Pavelka N, Berman J. 2019. Aneuploidy Enables Cross-
978 Adaptation to Unrelated Drugs. Mol Biol Evol 36:1768-1782.
979 Yang F, Todd RT, Selmecki A, Jiang YY, Cao YB, Berman J. 2021. The fitness costs and benefits of
980 trisomy of each Candida albicans chromosome. Genetics 218.
981 Yona AH, Manor YS, Herbst RH, Romano GH, Mitchell A, Kupiec M, Pilpel Y, Dahan O. 2012.
982 Chromosomal duplication is a transient evolutionary solution to stress. Proc Natl Acad Sci U S A
983 109:21010-21015.
984

985

986 Table 1. Karyotypes of SC5314 adaptors from passaging experiment

Passage number (day)	Selection pressure FLC (μg/ml)	Adaptor response	Number of sequenced adaptors	Genome features*
1	2	Tolerance	5	ChrRx3 (n=3); ChrRx3+Chr4x3 (n=1); segChrRx1 (from 1.89 Mb to right telomere, n=1)
5	128	Tolerance	2	ChrRx3
	1	Tolerance	1	ChrRx3
		Resistance	4	Euploid
	0.25	Tolerance	1	ChrRx3
		Resistance	5	Euploid
10	0.5	Tolerance	3	SegChrRx3 (from left telomere to 1.89MB, n=2); ChrRx3 +Chr7x3+Chr4x3 (n=1)
		Resistance	3	Chr5x3
	1	Tolerance	3	ChrRx3+Chr4x3 (n=1); ChrRx3+Chr6x3 (n=1); Chr6x3 (n=1)
		Resistance	3	Euploid
	2	Tolerant	6	ChrRx3+Chr4x3 (n=4); ChrRx3+Chr4x3+Chr2x3 (n=1); ChrRx3+Chr4x3+Chr6x3 (n=1)
	128	Tolerance	6	ChrRx3+Chr4x3
	0.25	Resistance	6	Euploid
	0.5	Resistance	6	Chr5x3 (n=2); Chr7x3 (n=1); Euploid (n=3)
15	1	Resistance	6	Chr3x3 (n=2); Chr7x3 (n=3); Chr7x3+Chr6x3 (n=1)
	2	Tolerance	6	SegChrRx3 (from left telomere to 1.89 MB, n=2); ChrRx3 (n=2); ChrRx3+Chr4x3 (n=2)
	128	Tolerance	6	SegChrRx3 (from left telomere to 1.89 MB, n=1); ChrRx3+Chr4x3 (n=5)

[*]See Fig. 7 and Fig. S6 for Ymap views of the karyotypes. Annotation such as “x3” indicates trisomy, “+” indicates additional aneuploidy in the same adaptor. n, number of isolates with this karyotype.

Figure 1

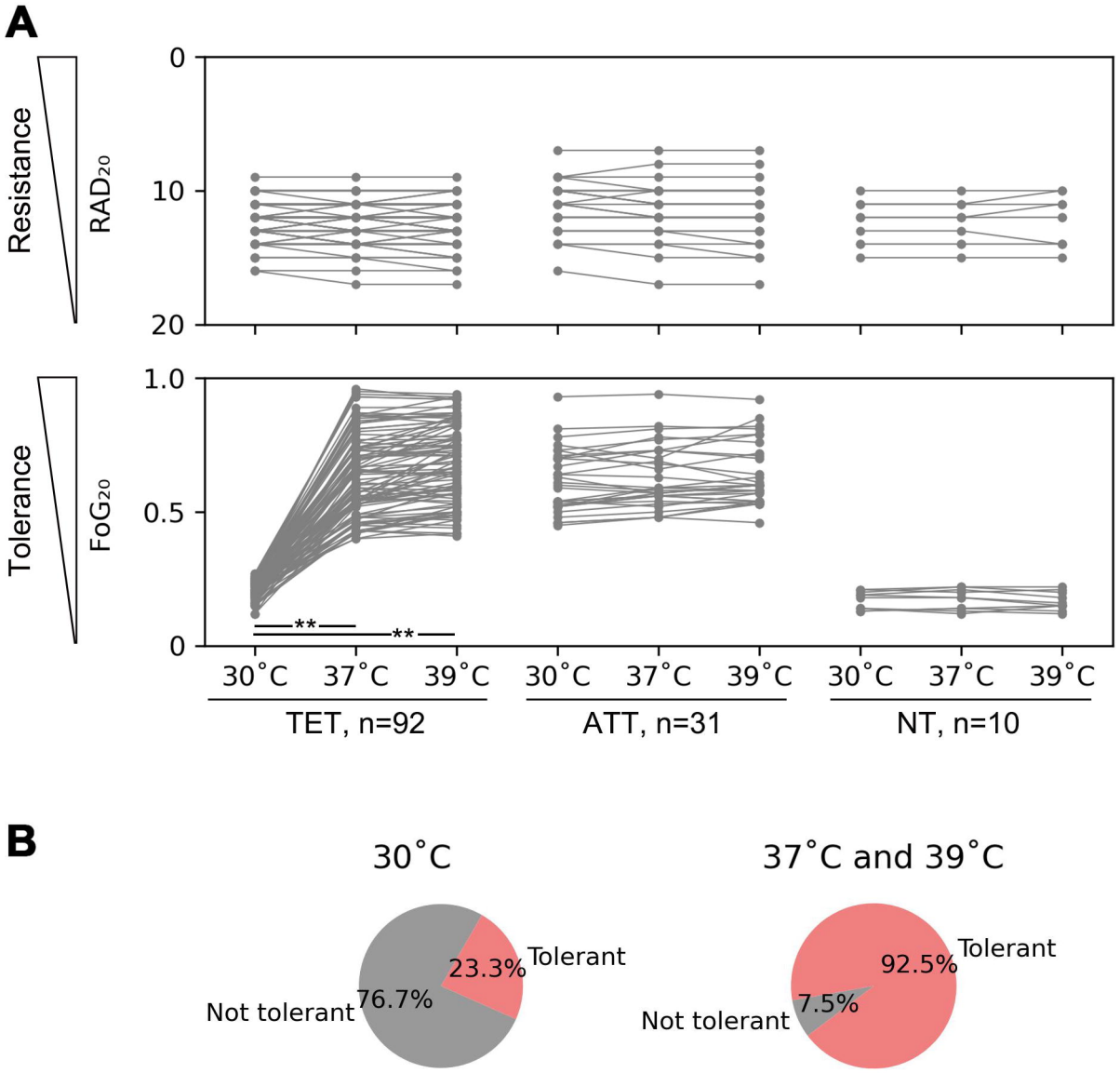
A
Resistance
RAD20
0
10
20
Tolerance
FoG20
1.0
0.5
0
**
**
30°C
37°C
39°C
30°C
37°C
39°C
30°C
37°C
39°C
TET, n=92
ATT, n=31
NT, n=10
B
30°C
23.3%
Tolerant
76.7%
Not tolerant
37°C and 39°C
92.5%
Tolerant
7.5%
Not tolerant

Figure 2

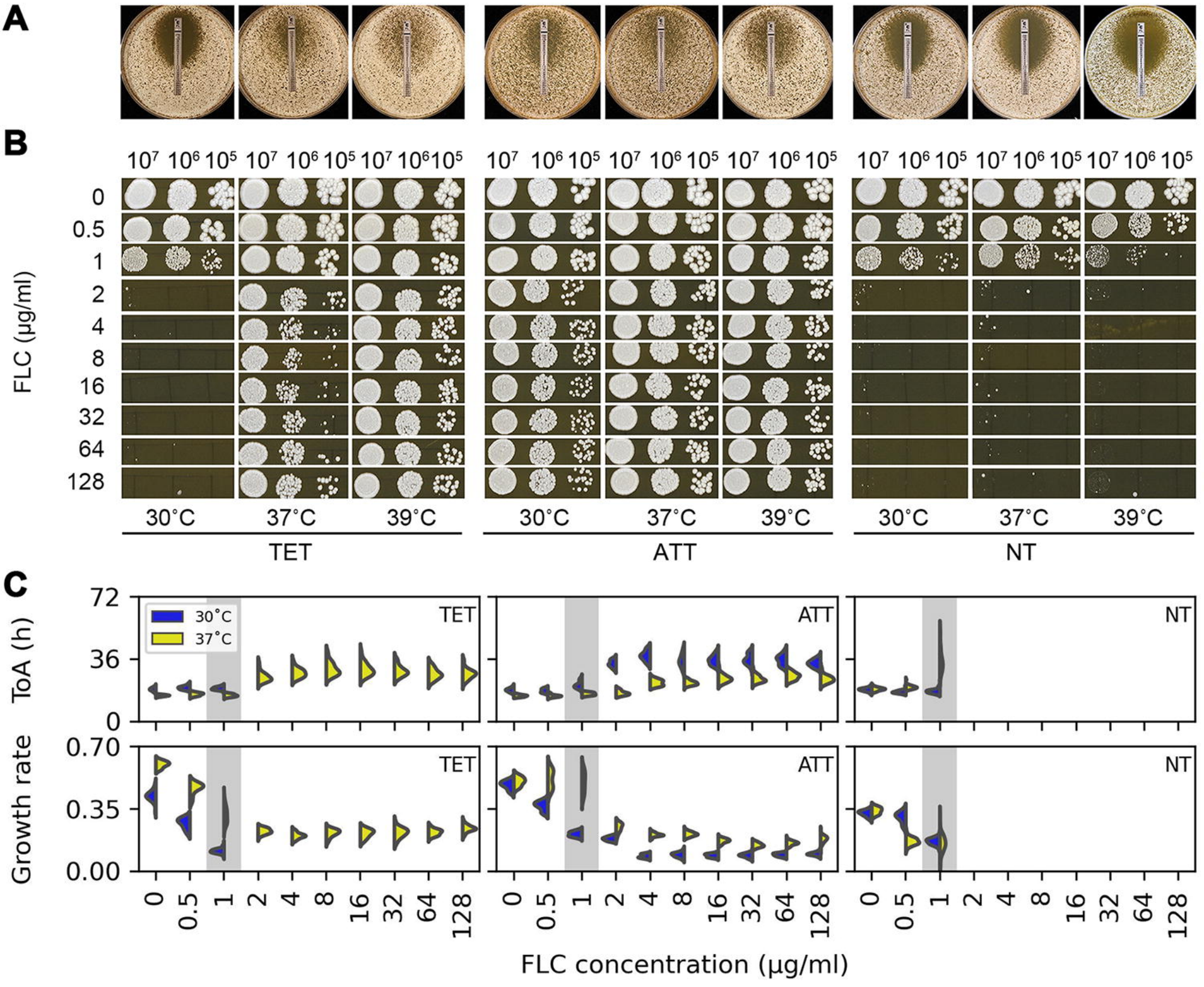
A
B
10^7 10^6 10^5 10^7 10^6 10^5 10^7 10^6 10^5
10^7 10^6 10^5 10^7 10^6 10^5 10^7 10^6 10^5
10^7 10^6 10^5 10^7 10^6 10^5 10^7 10^6 10^5
FLC (µg/ml)
0
0.5
1
2
4
8
16
32
64
128
30°C 37°C 39°C
30°C 37°C 39°C
30°C 37°C 39°C
TET
ATT
NT
C
ToA (h)
72
36
0
30°C
37°C
TET
ATT
NT
Growth rate
0.70
0.35
0.00
0 0.5 1 2 4 8 16 32 64 128
FLC concentration (µg/ml)

Figure 3

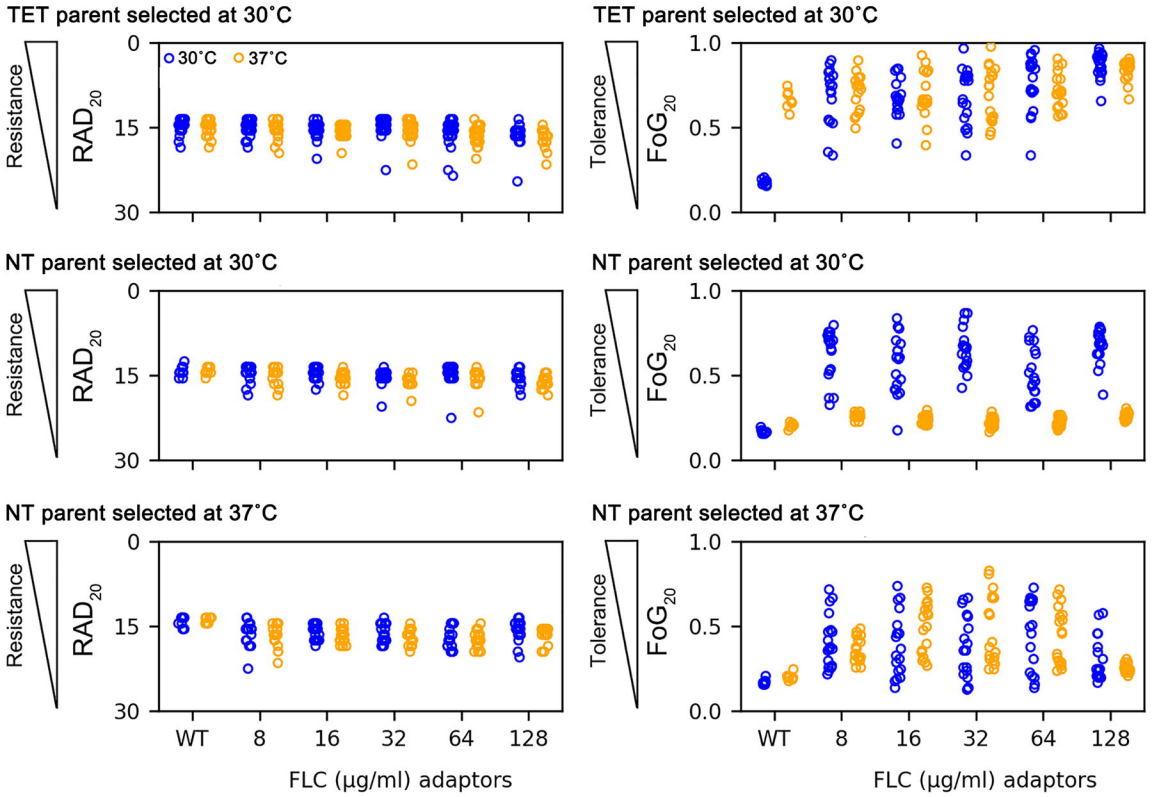
TET parent selected at 30˚C
NT parent selected at 30˚C
NT parent selected at 37˚C
Resistance
Tolerance
RAD20
FoG20
30˚C
37˚C
0
15
30
0.0
0.5
1.0
WT
8
16
32
64
128
FLC (µg/ml) adaptors

Figure 4

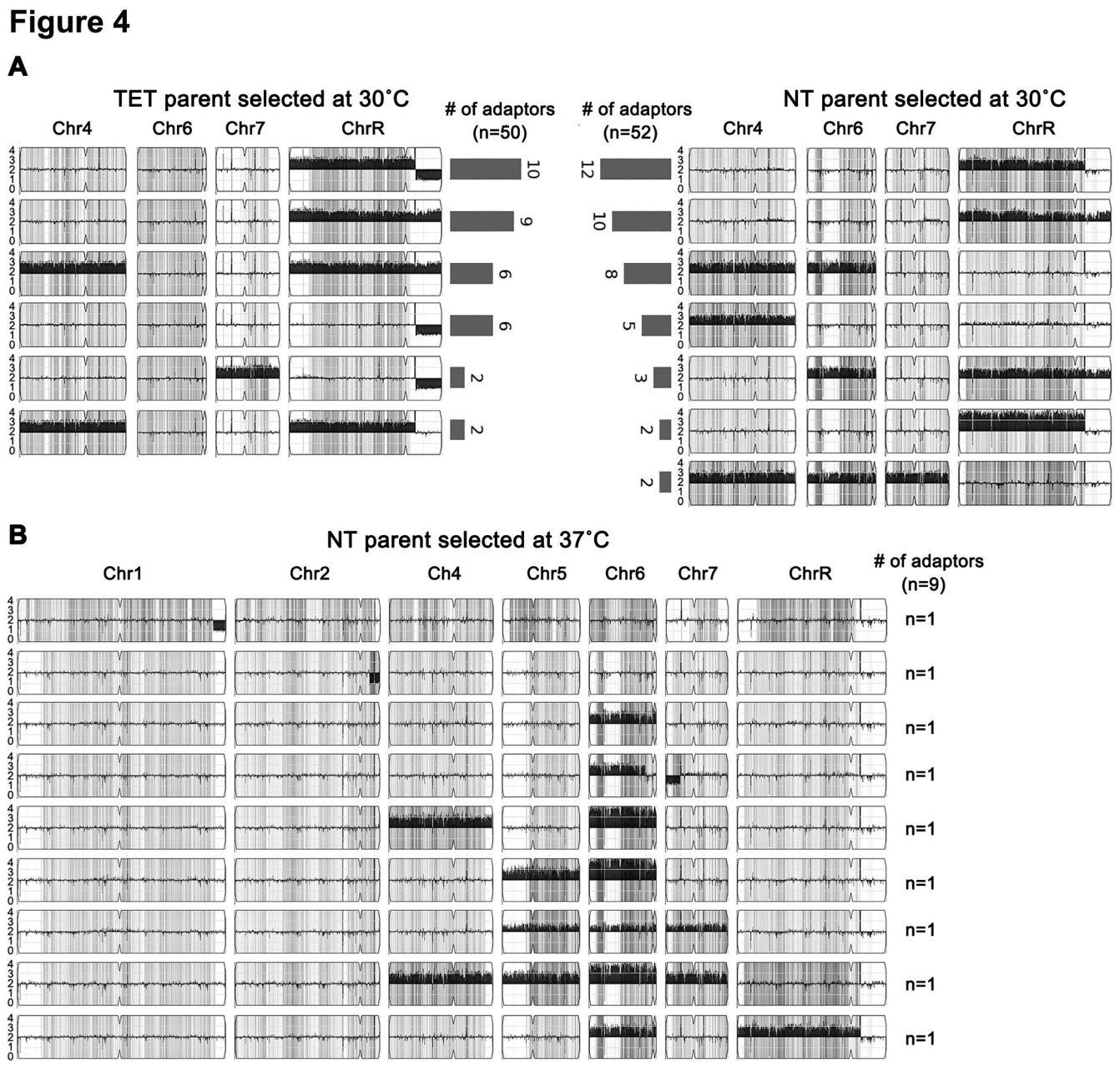
A
TET parent selected at 30˚C
Chr4
Chr6
Chr7
ChrR
# of adaptors (n=50)
10
9
6
6
2
2
# of adaptors (n=52)
12
10
8
5
3
2
2
NT parent selected at 30˚C
Chr4
Chr6
Chr7
ChrR
B
NT parent selected at 37˚C
Chr1
Chr2
Ch4
Chr5
Chr6
Chr7
ChrR
# of adaptors (n=9)
n=1
n=1
n=1
n=1
n=1
n=1
n=1
n=1
n=1

Figure 5

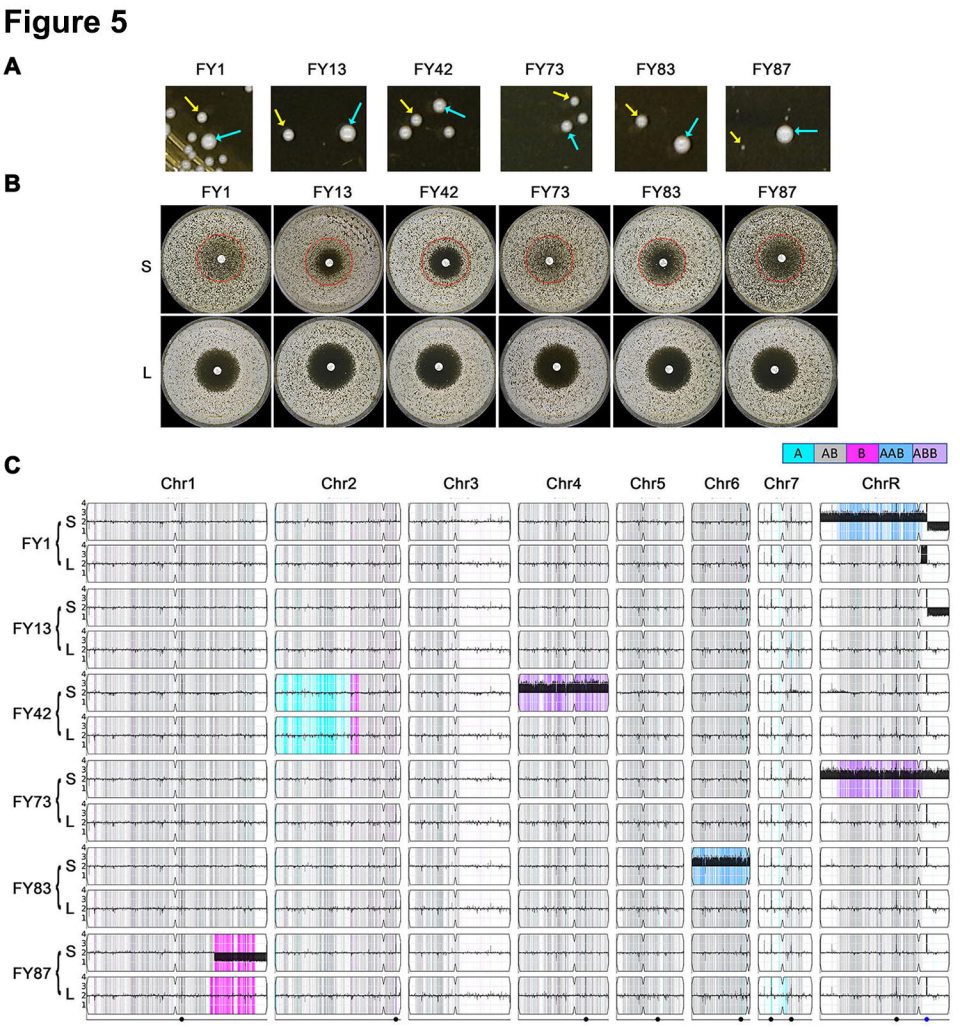
A
FY1
FY13
FY42
FY73
FY83
FY87
B
FY1
FY13
FY42
FY73
FY83
FY87
S
L
C
A
AB
B
AAB
ABB
Chr1
Chr2
Chr3
Chr4
Chr5
Chr6
Chr7
ChrR
FY1
FY13
FY42
FY73
FY83
FY87
S
L

Figure 6

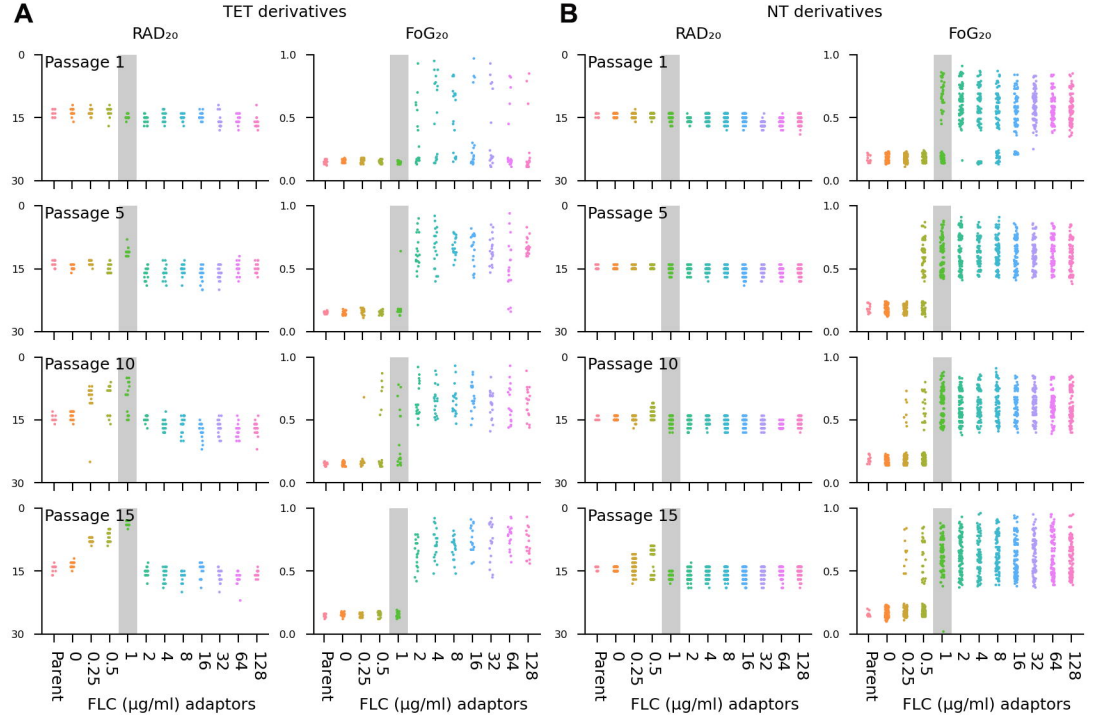
A
TET derivatives
RAD20
FoG20
B
NT derivatives
RAD20
FoG20
Passage 1
Passage 5
Passage 10
Passage 15
0
15
30
0.0
0.5
1.0
Parent
0
0.25
0.5
1
2
4
8
16
32
64
128
FLC (µg/ml) adaptors

Figure 7

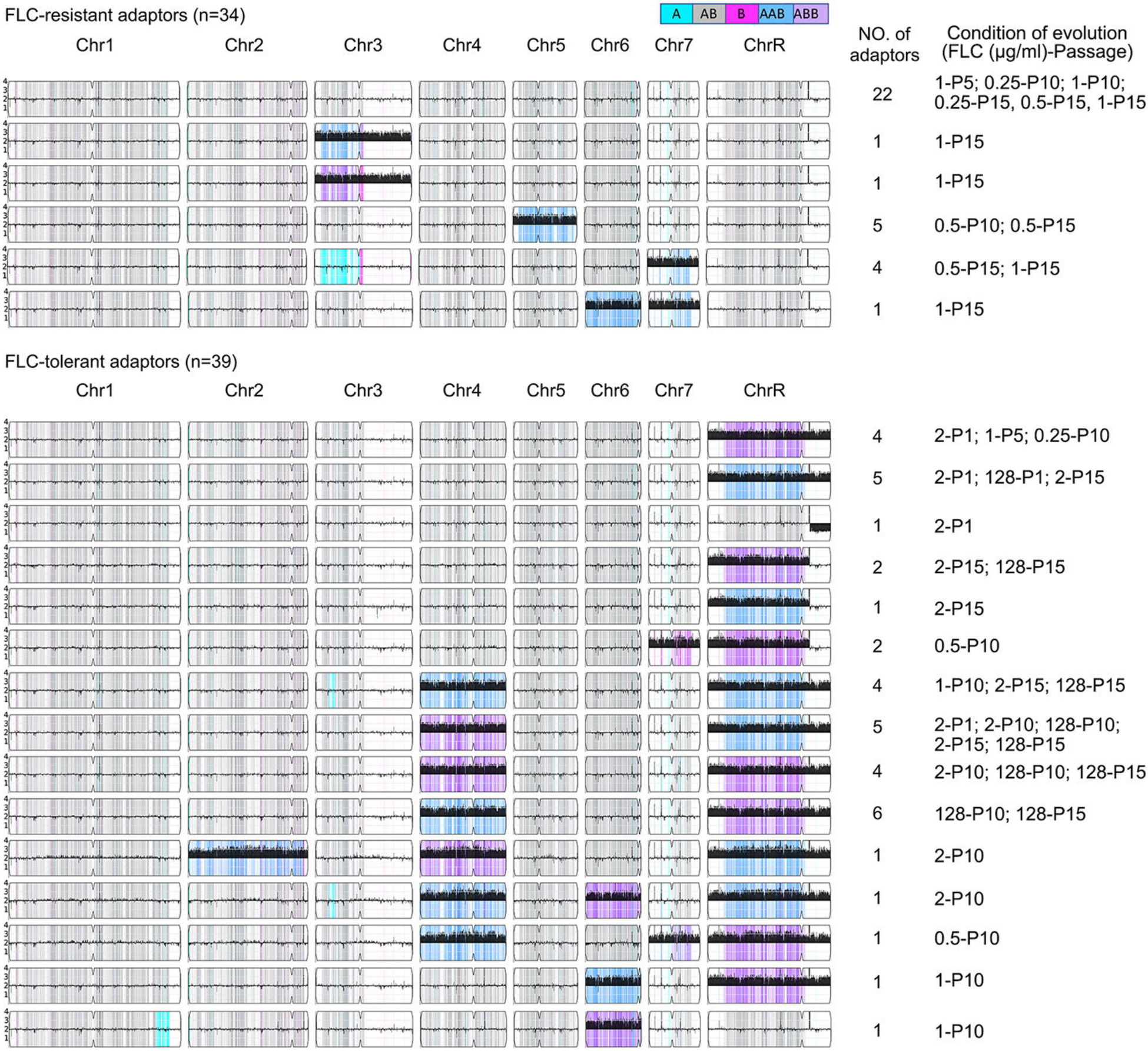
FLC-resistant adaptors (n=34)
A
AB
B
AAB
ABB
Chr1
Chr2
Chr3
Chr4
Chr5
Chr6
Chr7
ChrR
NO. of adaptors
Condition of evolution (FLC (μg/ml)-Passage)
22
1-P5; 0.25-P10; 1-P10; 0.25-P15, 0.5-P15, 1-P15
1
1-P15
1
1-P15
5
0.5-P10; 0.5-P15
4
0.5-P15; 1-P15
1
1-P15
FLC-tolerant adaptors (n=39)
Chr1
Chr2
Chr3
Chr4
Chr5
Chr6
Chr7
ChrR
4
2-P1; 1-P5; 0.25-P10
5
2-P1; 128-P1; 2-P15
1
2-P1
2
2-P15; 128-P15
1
2-P15
2
0.5-P10
4
1-P10; 2-P15; 128-P15
5
2-P1; 2-P10; 128-P10; 2-P15; 128-P15
4
2-P10; 128-P10; 128-P15
6
128-P10; 128-P15
1
2-P10
1
2-P10
1
0.5-P10
1
1-P10
1
1-P10